Supplementary Information: Boundary Design Regulates the Diffusion of Active Matter in Heterogeneous Environments

Kevin J. Modica,[a] Ahmad K. Omar,[b] and Sho C. Takatori*[a]

[a]Department of Chemical Engineering, University of California, Santa Barbara, Santa Barbara, CA 93106 USA.
[b]Department of Materials Science and Engineering, University of California, Berkeley, Berkeley, CA 94720 USA.
*Correspondence: Sho C. Takatori; stakatori@ucsb.edu

1 Appendix

1.1 Simulation Protocols

We implemented our simulations using HOOMD-blue, a molecular dynamics (MD) simulation package in Python[1]. We focused on the dilute limit of a single active Brownian particle (ABP) at position $\mathbf{R_i}$ and orientation θ_i. The ABPs have diameter σ in 2D and interact with fixed obstacles; therefore, hydrodynamic interactions are ignored in these simulations. The ABPs were initialized and simulated according to the overdamped Langevin equations of motion:

$$\frac{d\mathbf{R}_i}{dt} = \sqrt{2D_T}\eta_i(t) + \frac{\mathbf{F}_{i,rep}(\mathbf{R_i})}{\zeta} + \frac{\mathbf{F}_{i,swim}}{\zeta} \tag{1a}$$

$$\frac{d\theta_i}{dt} = \sqrt{2D_R}\xi_i(t). \tag{1b}$$

where $\mathbf{F}_{i,rep}$ is the repulsive force on particle i from the boundaries, ζ is the drag coefficient, and $\mathbf{F}_{i,swim}$ is the swim force. The swim force is set as $\mathbf{F}_{i,swim} = U_0\zeta\mathbf{q}_i$, where $\mathbf{q}_i = [\cos\theta_i, \sin\theta_i]$ is the unit vector describing particle i's orientation in 2D. Finally, the thermal and rotational diffusion coefficients are D_T and $D_R = 1/\tau_R$, with $(\eta_i,\ \xi_i)$ as random variables obeying the zero mean and variance consistent with the fluctuation-dissipation theorem. We integrate these equations using a timestep of $\Delta t = 0.001\sigma^2/D_T$ and integrate the equation over at least 10^7 steps. To obtain proper statistics, 10^4 ABPs were integrated per simulation. The drag coefficient and the energy scale of the potential were chosen such that the active force is much less than the repulsive force at contact $U_0\zeta \ll \frac{24\varepsilon}{\sigma}$, preventing significant overlap. Hard-sphere like interactions between the obstacles and the ABPs were implemented using the Weeks-Chandler-Andersen (WCA)[2] potential (Eq. 2). The boundaries of each system were formed using overlapping rigid surface particles also of size σ. These surface particles are offset to define the boundaries of the system as the location the ABPs are at contact with the surface particles (the ABP center is a distance σ from the wall surface particle's center). The repulsive force from the boundaries on active particle i is given by

$$\mathbf{F}_{i,rep} = -\nabla V_{i,wca} \tag{2a}$$

$$V_{wca}(\mathbf{R_i}) = \sum_j \begin{cases} 4\varepsilon\left[\left(\frac{\sigma}{r_{ij}}\right)^{12} - \left(\frac{\sigma}{r_{ij}}\right)^{6}\right] + \varepsilon,\ r_{ij} \le 2^{1/6}\sigma. \\ 0,\ r_{ij} > 2^{1/6}\sigma. \end{cases} \tag{2b}$$

Where $r_{ij} = \|\mathbf{R_i} - \mathbf{R_j}\|$ represents the pairwise distance between the ABP at position $\mathbf{R_i}$ and the rigid surface particles at position $\mathbf{R_j}$. The particle diameters were chosen to be small compared to the geometric features of the obstacle ($\sigma \ll R, H, L$ etc.).

1.2 Generalized Taylor Dispersion Theory (GTDT) Derivation for a Square Lattice

We use generalized Taylor dispersion theory to obtain the effective translational diffusivity of active particles in an array of hard obstacles using established procedures[3–9]. $P(\mathbf{R},\mathbf{q},t)$ represents the probability distribution of an active particle with position $\mathbf{R}$ and orientation $\mathbf{q}$ moving through a lattice. There are two local variables, the orientation vector $\mathbf{q}$, and the radial coordinate $\mathbf{r} = \mathbf{R} - \mathbf{X}$ which is defined as the distance to the nearest lattice center at location $\mathbf{X}$.

$$\mathbf{R} = \mathbf{X} + \mathbf{r} \tag{3}$$

While $\mathbf{X} = N_L\mathbf{L}$ is strictly a discrete variable defined in terms of the lattice spacing $\mathbf{L}$ and the lattice number N_L, we can approximate it as a continuous variable for our purposes due to our interest in the far field effects ($\mathbf{X} \gg \mathbf{L}$).

$$\frac{\partial P(\mathbf{X},\mathbf{r},\mathbf{q},t)}{\partial t} + \nabla_X \cdot \mathbf{J} + \nabla_r \cdot \mathbf{J} - D_R \frac{\partial^2 P}{\partial \theta^2} = 0 \tag{4}$$

$$\mathbf{J} = U_0 \mathbf{q} P - D_T (\nabla_X P + \nabla_r P) \tag{5}$$

We now obtain the average flux of the active particle in Fourier space $\big(\mathbf{X} \to \mathbf{k}$, and $P(\mathbf{X},\mathbf{r},\mathbf{q},t) \to \hat{P}(\mathbf{k},\mathbf{r},\mathbf{q},t)\big)$. Then, we integrate over local degrees of freedom to get the Fourier transformed macroscopic number density $\hat{n}(\mathbf{k},t) = \langle \hat{P} \rangle_{q,r}$.

$$\frac{\partial \hat{n}(\mathbf{k},t)}{\partial t} + i\mathbf{k} \cdot \langle \hat{\mathbf{j}}_{\mathbf{1}} \rangle_{q,r} = 0 \tag{6a}$$

$$\langle \hat{\mathbf{j}}_{\mathbf{1}} \rangle_{q,r} = \hat{n}(\mathbf{k},t)[\mathbf{u_E} - i\mathbf{k} \cdot \mathbf{D_E}] \tag{6b}$$

To achieve expressions for the average effective velocity ($\mathbf{u_E}$) and diffusivity ($\mathbf{D_E}$), we define the structure function $\hat{G}$ as the full probability distribution divided by the macroscopic number density and then expand the structure function in low wave-vectors:

$$\hat{P}(\mathbf{k},\mathbf{r},\mathbf{q},t) = \hat{n}(\mathbf{k},t)\hat{G}(\mathbf{k},\mathbf{r},\mathbf{q},t) \tag{7a}$$

$$\hat{G}(\mathbf{k},\mathbf{r},\mathbf{q},t) = g_0(\mathbf{r},\mathbf{q},t) + i\mathbf{k} \cdot \mathbf{d}(\mathbf{r},\mathbf{q},t) + \mathscr{O}(\mathbf{kk}). \tag{7b}$$

After substituting into Eq. 4 we derive the governing equations for the microstructure field $g_0(\mathbf{r},\mathbf{q},t)$ and fluctuation field $\mathbf{d}(\mathbf{r},\mathbf{q},t)$:

Microstructure Field

$$\frac{\partial g_0(\mathbf{r},\mathbf{q},t)}{\partial t} + \nabla_r \cdot [U_0 \mathbf{q} g_0 - D_T \nabla_r g_0] - D_R \frac{\partial^2 g_0}{\partial \theta^2} = 0 \tag{8a}$$

$$\hat{\mathbf{n}} \cdot [U_0 \mathbf{q} g_0 - D_T \nabla_r g_0] = 0, \text{ on the obstacle surface} \tag{8b}$$

$$\langle g_0(\mathbf{r},\mathbf{q}) \rangle_{r,q} = 1 \tag{8c}$$

Fluctuation Field:

$$\begin{aligned} \frac{\partial \mathbf{d}(\mathbf{r},\mathbf{q},t)}{\partial t} &+ \nabla_r \cdot [U_0 \mathbf{q} \mathbf{d} - D_T (\mathbf{I} g_0 + \nabla_r \mathbf{d})] \\ -D_R \frac{\partial^2 \mathbf{d}}{\partial \theta^2} &= -[U_0 \mathbf{q} g_0 - D_T \nabla_r g_0] \end{aligned} \tag{9a}$$

$$\hat{\mathbf{n}} \cdot [U_0 \mathbf{q} \mathbf{d} - D_T (\mathbf{I} g_0 + \nabla_r \mathbf{d})] = \mathbf{0}, \text{ on the obstacle surface} \tag{9b}$$

$$\langle \mathbf{d}(\mathbf{r},\mathbf{q}) \rangle_{r,q} = \mathbf{0} \tag{9c}$$

Where $\hat{\mathbf{n}}$ is the unit normal of the obstacle boundary. Both the microstructure and fluctuation fields are subject to periodic boundary conditions in rotation and across unit cell boundaries. This method provides definitions for the effective velocity and diffusivity in terms of the microstructure and fluctuation fields.

$$\mathbf{u_E} = U_0 \langle \mathbf{q} g_0 \rangle_{q,r} - D_T \langle \nabla_r g_0 \rangle_{q,r} \tag{10}$$

$$\mathbf{D_E} = D_T \mathbf{I} - U_0 \langle \mathbf{q} \mathbf{d} \rangle_{q,r} + D_T \langle \nabla_r \mathbf{d} \rangle_{q,r} \tag{11}$$

For all these systems, there is no net drift and as such the effective velocity is zero. From Eq. 11 the effective diffusivity tensor is determined by integrating dyads of the fluctuation field with the orientation vector or the gradient operator. Taking the *integrand* of the translational integral in Equation 11 allows one to gain local information on how the diffusivity is impacted by the obstacle.

$$\mathbf{D_E} = \left\langle \frac{D_T}{\Omega}\mathbf{I} - U_0\langle \mathbf{qd}\rangle_q + D_T\langle \nabla_r \mathbf{d}\rangle_q \right\rangle_r \tag{12}$$

We define the local diffusivity such that its *average* is equal to the value obtained in Equation 11 and therefore we multiply all terms by Ω:

$$D_{xx}(\mathbf{r}) = D_T - \Omega U_0 \langle q_x d_x\rangle_q + \Omega D_T \left\langle \frac{\partial}{\partial x} d_x \right\rangle_q \tag{13a}$$

$$D_{E,xx} = \frac{1}{\Omega}\langle D_{xx}(\mathbf{r})\rangle_r \tag{13b}$$

$$D_{yy}(\mathbf{r}) = D_T - \Omega U_0 \left\langle q_y d_y\right\rangle_q + \Omega D_T \left\langle \frac{\partial}{\partial y} d_y \right\rangle_q \tag{13c}$$

$$D_{E,yy} = \frac{1}{\Omega}\left\langle D_{yy}(\mathbf{r})\right\rangle_r \tag{13d}$$

where Ω is the free space unoccupied by the obstacle inclusion. In the square lattice array the average effective diffusivities are the same: $D_{E,xx} = D_{E,yy} = D_E$. For the sinusoidal pore or the tortuous path there are hard boundaries blocking motion in the x direction: $D_{E,xx} = 0$, $D_{E,yy} = D_E$.

1.3 Derivation of Fick-Jacobs Approximation for Active Matter

We start with the Smoluchowski equation for an active particle moving in two dimensions under an external potential $V(y)$.

$$\frac{\partial P(x,y,\mathbf{q},t)}{\partial t} + \nabla\cdot\left[U_0\mathbf{q}P - D_T\nabla P - \frac{D_T}{k_BT}P\nabla V\right] - D_R\frac{\partial^2 P}{\partial\theta^2} = 0 \tag{14}$$

We can treat this external potential as an free energy penalty imposed by reduction in entropy from the pore constricting and expanding: $V(y) = -k_BT\ln(w(y))$.

$$\frac{\partial P(x,y,\mathbf{q},t)}{\partial t} + \nabla\cdot\left[U_0\mathbf{q}P - D_T\nabla P + D_T P\nabla\ln(w)\right] - D_R\frac{\partial^2 P}{\partial\theta^2} = 0 \tag{15}$$

To find the diffusion coefficient along the pore using the Fick-Jacobs equations, we define the averaged distribution as:

$$M(y,\mathbf{q},t) = \frac{1}{w(y)}\int_{x=-\frac{w(y)}{2}}^{x=\frac{w(y)}{2}} P(x,y,\mathbf{q},t)\,d\mathrm{x} \tag{16}$$

Where $-w(y)/2$ is the x position at the left hand side of the pore, and $w(y)/2$ is the x position at the right hand side of the pore. Following the methods of Sandoval and Dagdug[10], we integrate the Smoluchowski equation over x to isolate the axial motion.

For a very thin channel we can approximate the motion as quasi-1D in y and ignore variations in x, $P(x,y,\mathbf{q},t)\to P(y,\mathbf{q},t)$. Substituting that into Eq. 16:

$$M(y,\mathbf{q},t) = P(y,\mathbf{q},t). \tag{17}$$

Finally, after simplifying Eq. 15 subject to Eq. 17 we arrive at:

$$\frac{\partial M}{\partial t} + U_0\sin\theta\frac{\partial M}{\partial y} - \frac{\partial}{\partial y}\left[D_T\frac{\partial M}{\partial y} - D_T M\frac{\partial\ln w}{\partial y}\right] - D_R\frac{\partial^2 M}{\partial\theta^2} = 0. \tag{18}$$

Previous work by Rubí and Reguera[11] demonstrated that these solutions can be improved by the introduction of a spatially varying diffusion coefficient $D(y)$

$$D(y) = \frac{D_T}{[1+(1/4)w'(y)^2]^{1/3}}. \tag{19}$$

This can be generalized by mapping the active case onto it's passive equivalent[10]:

$$D(y) = \frac{D_0}{[1 + (1/4)w'(y)^2]^{1/3}}. \tag{20}$$

Finally, the effective diffusivity can be estimated by averaging the spatially varying diffusion coefficient over the periodic system using the Lifson-Jackson formula[12].

$$D_E = \frac{1}{\langle w(y)\rangle} \frac{1}{\langle 1/D(y)w(y)\rangle} \tag{21}$$

1.4 Contours for a Narrow Pore Found via Taylor Dispersion Theory

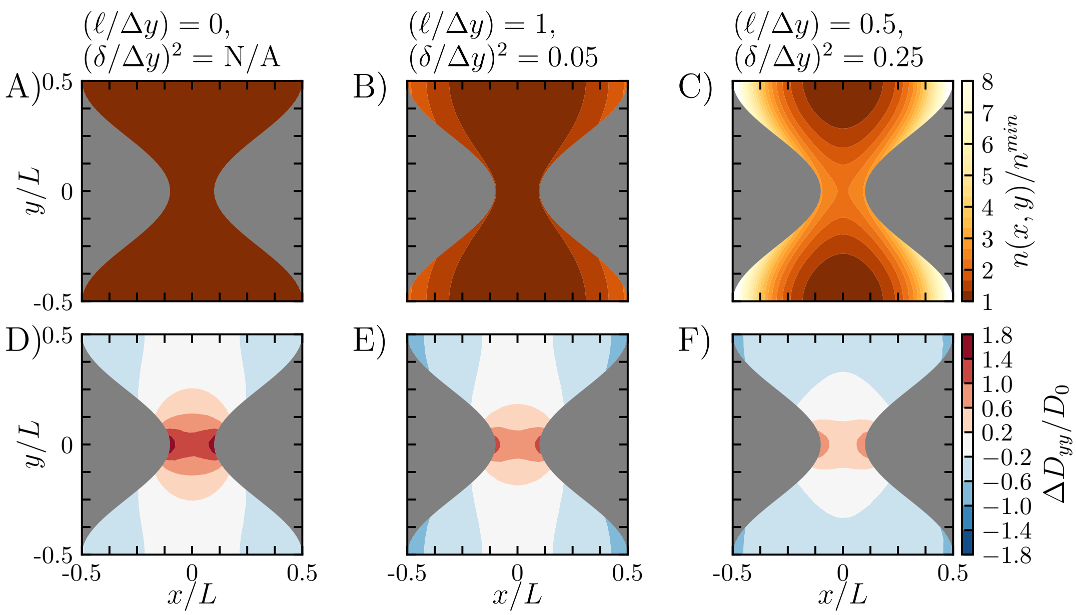

Fig. 1 Particles accumulate in concave regions. A-C Local number density of particles for different activity parameters. As the activity increases in strength, the particles experience larger accumulation near the obstacle surface as shown through the contours. **D-F** The pointwise diffusivity deviation found via GTDT (not Fick-Jacobs) along the y direction is $\Delta D_{yy}/D_0 = \left(D_{yy}(\mathbf{r}) - D_{\text{Model}}\right)/D_0$. The pointwise diffusivity along the y direction is calculated numerically via dispersion theory. As activity increases, the ABPs spend more time in the convex region with low local diffusivity, reducing the throughput at the narrow escape. Subplots **A,D** correspond to $\ell/R = 0$ and $\delta^2/R^2 = \mathrm{N/A}$. Subplots **B,E** correspond to $\ell/\Delta y = 1$ and $(\delta/\Delta y)^2 = 0.05$. Subplots **C,F** correspond to $\ell/\Delta y = 0.5$ and $(\delta/\Delta y)^2 = 0.25$. All data collected for $(H-b)/H = 0.8$

.

1.5 Additional Measurements of ABP Diffusivity through a Tortuous Path

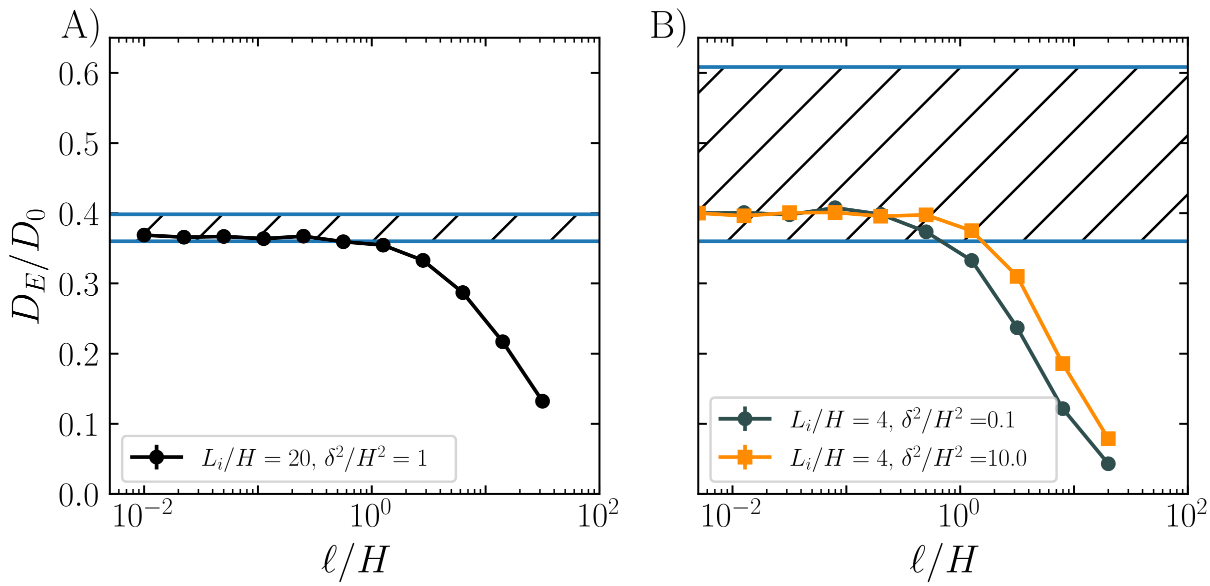

Fig. 2 Additional scaled effective diffusivity measurements of active particles confined to a tortuous path. **A**) The tortuosity scaling prediction begins to fail at $\ell/H \approx 1$, even for paths of very large aspect ratio $L_i/H = 20$. This indicates that the geometric feature of interest is H, the smallest length scale in this geometry. **B**) The scaled diffusivity is relatively insensitive to the microscopic length, justifying our use of several different $(\delta/H)^2$ ratios when spanning the parameter space in the main text.

References

1 J. A. Anderson, J. Glaser and S. C. Glotzer, *Computational Materials Science*, 2020, **173**, 109363.

2 J. D. Weeks, D. Chandler and H. C. Andersen, *The Journal of Chemical Physics*, 1971, **54**, 5237–5247.

3 S. C. Takatori and J. F. Brady, *Soft Matter*, 2014, **10**, 9433–9445.

4 R. N. Zia and J. F. Brady, *Journal of Fluid Mechanics*, 2010, **658**, 188–210.

5 M. Mangeat, T. Guérin and D. S. Dean, *The Journal of Chemical Physics*, 2020, **152**, 234109.

6 S. C. Takatori and J. F. Brady, *Physical Review Letters*, 2017, **118**, 018003.

7 Z. Peng and J. F. Brady, *Physical Review Fluids*, 2020, **5**, 073102.

8 E. W. Burkholder and J. F. Brady, *Physical Review E*, 2017, **95**, 052605.

9 R. Alonso-Matilla, B. Chakrabarti and D. Saintillan, *Physical Review Fluids*, 2019, **4**, 043101.

10 M. Sandoval and L. Dagdug, *Physical Review E - Statistical, Nonlinear, and Soft Matter Physics*, 2014, **90**, 062711.

11 D. Reguera and J. M. Rubí, *Physical Review E*, 2001, **64**, 061106.

12 S. Lifson and J. L. Jackson, *The Journal of Chemical Physics*, 1962, **36**, 2410–2414.